*Materials Science Forum Vols. 495-497 (2005) pp 393-398*
*online at http://www.scientific.net*

*Online available since 2005/Sep/15*



# An EBSD Investigation on Deformation-Induced Shear Bands In Ti-Bearing IF-Steel Under Controlled Shock-Loading Conditions

J.F.C. Lins[1,a], H.R.Z. Sandim[1,b], K.S. Vecchio[2,c] and D. Raabe[3,d]

[1]Departamento de Engenharia de Materiais, FAENQUIL, P.O. Box 116, Lorena, São Paulo, 12600-970, Brazil

[2]Department of Mechanical and Aerospace Engineering, University of California, San Diego, La Jolla, CA 92093-0411, USA

[3]Max-Planck-Institut für Eisenforschung, Max-Planck-Straβe 1, Düsseldorf, 40237, Germany

[a]fabricio.lins@ppgem.faenquil.br, [b]hsandim@demar.faenquil.br, [c]kvecchio@ucsd.edu, [d]raabe@mpie.de

**Keywords:** IF steel, adiabatic shear bands, EBSD, recrystallization, and microtexture.

**Abstract.** We report the results of the microstructural characterization of a Ti-bearing IF-steel deformed at high strain rates ($\approx 6.10^4$ $s^{-1}$) in a split Hopkinson bar. The shock-loading tests were performed in hat-shaped specimens to induce the formation of adiabatic shear bands (ASB). The samples were deformed at 223 K and 298 K. High-resolution electron backscatter diffraction (EBSD) reveals the development of an ultrafine-grained structure within the ASB. A closer inspection reveals the presence of deformation twins in grains adjacent to the shear band. These twins bend towards the ASB suggesting that mechanical twinning occurs before the flow associated to shear banding. The results of microtexture have indicated the presence of a sharp <111> γ-fiber texture in the ASB for both temperatures.

## Introduction

Shock loading experiments have been performed in carbon steels and many other materials over the last decades [1]. Metals can be processed at high strain rates in several operations like high-speed machining, metal forming, and ballistic impact tests. In most cases, depending on the applied strain rate, they tend to display regions of highly localized straining. It is worth mentioning that during the short time of the shock-loading impact (in the range of μs), the amount of heat generated is confined in the shear band and is not dissipated to the vicinity of the band [1,2]. For this reason, this highly localized process is considered adiabatic for practical purposes.

ASB in metals have been reviewed in the literature due to academic, military, and industrial concerns [1]. The metallographic inspection of shear regions has been mostly performed by transmission electron microscopy (TEM) in small areas. Therefore, TEM provides limited statistical information on the developed mesotexture. Only a few studies using conventional EBSD are reported in the literature in ASB due to an intrinsic limitation of the technique (low spatial resolution) [3,4]. In contrast, high-resolution EBSD is able to resolve the microstructure of severely deformed metals in relatively large areas compared to TEM. The use of an EBSD system coupled to a field emission gun (FEG) SEM improves the spatial resolution allowing determining misorientations of grains or subgrains as small as 0.1-0.2 μm in highly-deformed materials [5].

The final texture developed in IF steels is characterized by a sharp and homogeneous {111}<*uvw*> texture (γ-fiber) with components like {554}<225>, {554}<135>, and {111}<110> [6]. The γ-fiber in bcc metals comprises orientations where {111} planes are parallel to the normal direction (ND). At high rolling strains shear bands become prominent in many metals and play an important role in determining the deformation texture. It is also well known that these deformation

heterogeneities are favorable nucleation sites for recrystallization. Furthermore, investigating the microstructural evolution of ASB could give further information on the development of the deformation texture and the mechanical behavior at large strains in Ti-stabilized IF steels.

The aim of this work is to investigate the microstructure of ASBs induced by shock loading in a hot-band IF steel deformed to large strains with aid of a split Hopkinson bar at 223 K and 298 K. The microstructural characterization of deformed specimens was performed using scanning electron microscopy (SEM). High-resolution EBSD coupled to a field emission gun scanning electron microscope (FEG-SEM) was employed to investigate the shear region in great detail.

## Experimental Procedure

**Material.** CSN (Brazil) supplied the plate of the Ti-stabilized IF-steel used in this investigation. A 250-mm wide, 300-mm long plate was obtained by hot rolling in multiple passes in the austenitic field (1343 K) followed by air-cooling. The thickness of the steel plate was 38 mm. The total strain (ε) during the hot-rolling stage was about 2.2. The chemical composition of this ferritic steel (in wt.%) is 0.003 C, 0.069 Ti, 0.001Nb, 0.003 V, 0.049 Al, 0.0025 N, 0.005 O, 0.19 Mn, 0.011 Si, 0.027 P, and 0.005 S.

**Dynamic compression tests.** The dynamic compression tests were carried out in a split Hopkinson bar using hat-shaped specimens, as shown in Fig. 1. The cylindrical specimens were machined from the Ti-stabilized IF steel plate in such a manner that the ND of the hot-band was parallel to the hat's longitudinal axis. AISI 4340 stopper rings (SR) were used to control the shear strain (γ) in the material. The shear strain was determined by the ratio between the measured displacement (δ) and the thickness of the shear band (ξ). The thickness (ξ) of each ASB was measured using electron channeling contrast in SEM in the backscattered electrons mode. The total displacement (δ) was calculated by the difference between $h_1$ and final $h_3$ dimensions of the hat's height. Table 1 shows the corresponding dimensions of the samples and the conditions used in the shock-loading tests.

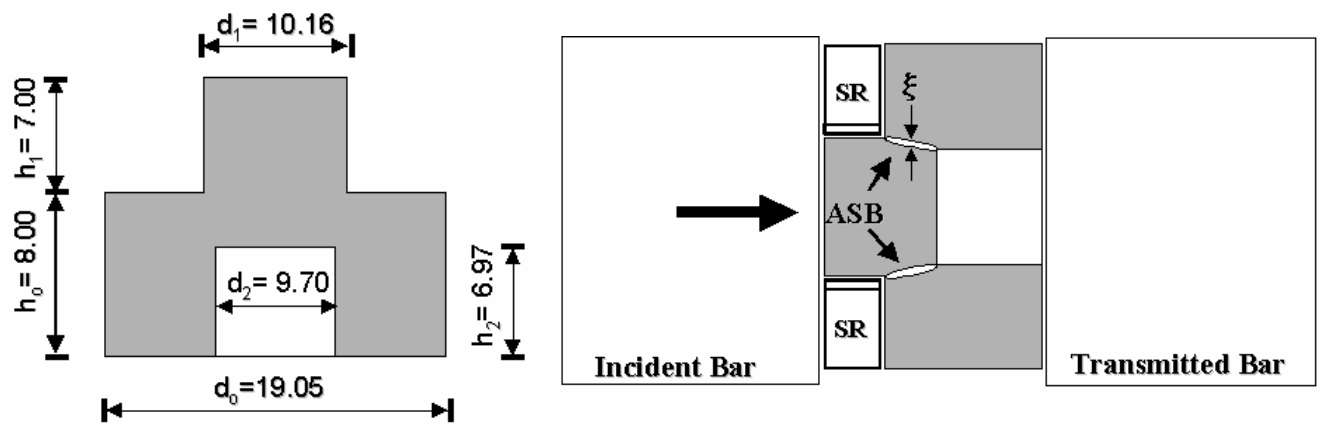


**Fig. 1** – Cross-section schematic drawing of the hat-shaped specimen used in this investigation (dimensions are given in mm). SR refers to the stopper ring and the thickness of the ASB is given by ξ.

**Table 1 –** Dimensions of the samples shown in Fig. 1 and the conditions used in the tests.

| *Sample* | $h_0$ | $d_0$ | $h_1$ | $d_1$ | $h_2$ | $d_2$ | $h_3$ | SR | Temperature [K] | Time [μs] | Strain rate [$10^4 s^{-1}$] |
|---|---|---|---|---|---|---|---|---|---|---|---|
| | [mm] | | | | | | | | | | |
| *S-1* | *8.13* | *19.05* | *6.88* | *10.16* | *7.26* | *9.68* | *4.95* | *5.00* | *223* | *122* | *5.59* |
| *S-2* | *7.85* | | *7.04* | | *7.01* | | *4.98* | | *298* | | *6.38* |

**Microstructural characterization.** Electron channeling contrast micrographs of the shock-loaded specimens were determined in a LEO 1450-VP SEM. The respective local texture developed within ASB was evaluated using the EBSD technique and orientation imaging microscopy (OIM). The high-resolution EBSD maps were performed in a JEOL JSM-6500F FEG-SEM operating at 15 kV also interfaced to a TSL package system. Metallographic preparation of the specimens was carried out using conventional techniques and the final chemical etching was done using an acid solution ($95H_2O_2$: 5HF) for 5 s.

## Results and Discussion

**Starting material.** The Ti-stabilized IF steel plate was evaluated in terms of its microstructure and texture in a previous work [7]. Results showed a weak and diffuse (random) texture in the hot band. The mean recrystallized grain size is 55 ± 6 μm.

**Deformed state.** The measured shear width of the samples is shown in Table 2. This table also presents the calculated values and expressions of the shear ($\gamma$) and longitudinal ($\varepsilon$) strains. As a general trend, the shear strain increases with the decrease of both the test temperature and shear width ($\xi$). The literature reported that the shear strain varies along the thickness of the shear band. Chen *et al.* [8] pointed out the problems that arise when ξ is measured. Due to a highly localized deformation (localized damage) at upper and lower areas of the hat-shaped specimen this measure is considered as a relative approach. This could be a reasonable explanation for the differences of calculated shear strain between deformed specimens.

**Table 2 –** Deformation parameters for the impacted specimens.

| Sample | Temperature [K] | $\delta$ [mm] | $\xi$ [μm] | $\gamma = \frac{\delta}{\xi}$ | $\varepsilon = \ln\left(\frac{\gamma^2}{2} + \gamma + 1\right)^{1/2}$ |
|---|---|---|---|---|---|
| *S-1* | *298* | *2.06* | *126.30* | *16.30* | *2.50* |
| *S-2* | *223* | *1.88* | *80.90* | *23.25* | *2.85* |

Fig. 2 shows a general view of the shear region induced in sample S-1. The ASB is positioned in the center of the map with the shear direction (SD) parallel to horizontal direction. The shear plane normal (SPN) is located parallel to vertical direction. This micrograph shows the morphology of the shear band (irregular shape) as well as the degree of subdivision of the neighboring grains. The fragmented grains adjacent to the ASB display deformation twins in most grains and long-range internal stresses associated to lattice rotations independent of their initial orientation.

Twinning is very sensitive to temperature and strain rate conditions [9]. In our experiments the conditions imposed to the material during deformation favored the occurrence of deformation twinning as an alternative deformation mode to dislocation slip. Most of the deformation twins display a typical lenticular morphology, independently of the test temperature. It was observed in all samples that twins were distributed randomly in the grain interior. A closer inspection reveals the presence of bowed twins in grains adjacent to the ASB (marked by arrows in Fig. 2). These twins are found bending towards the ASB suggesting that mechanical twinning occurs before the flow associated to shear banding. A similar feature was also reported for α-Ti deformed at large strain rates [10].

SEM shows a fine-grained structure in the central region of the ASB. These new equiaxed grains are surrounded by a well-developed lamellar structure, typically found in metals deformed to large strains. The width of the region displaying a recrystallized structure is about 35 μm. High-resolution EBSD was employed to investigate the microstructure in detail. A small step size (0.05 μm) was used to perform this orientation mapping. Results show the presence of regions with low density of defects resembling grains within the lamellar structure as can be clearly identified by the image

quality (IQ) map (not shown in this paper). The average misorientation associated to the boundaries found in the lamellar structure is about 55° (high-angle character) and are marked by black lines in the OIM (Fig. 3a). The lamellae spacing found in the shear band is about 0.3-0.2 μm. The orientation distribution function (ODF) of the recrystallized grains within the ASB indicated a clear and strong γ-fiber texture and a weak α-fiber (Fig. 3b). The average grain size is about 0.42 μm. The striking aspect in these findings is the similarity between the texture displayed by recrystallized grains within the ASB and the recrystallization texture reported in IF steels processed by severe cold rolling followed by isothermal annealing.

The information provided by high-resolution EBSD strongly suggests the occurrence of recrystallization (at least partial) in this material. A possible mechanism to explain the formation of this grain structure within the ASB is the rotational dynamic recrystallization postulated by *Derby* in [11]. Several authors suggest the occurrence of rotational dynamic recrystallization within shear bands in many metals like copper, tantalum, brass, steels, and titanium [4]. The microstructural evolution involved in this mechanism can be described as follows: i) rearrangement of the dislocations with increasing strain into elongated cells; ii) the thermal activation provided by the temperature rise and the development of increasing misorientations upon high-strain-rate straining transform these cells into an elongated subgrain structure bounded by many high-angle lamellar boundaries; iii) the final step proposed in this mechanism is the subdivision of these subgrains with the creation of geometrically necessary boundaries associated to a local crystal rotation. Meyers *et al.* [4] reported that the relaxation of the broken-down elongated subgrains into an equiaxed grain structure could occur by minor rotations of the grain boundaries. The estimate of the temperature rise during dynamic compression of this Ti-stabilized IF steel is in progress. For instance, literature reports a temperature rise of about 600°C for a 304-L stainless steel deformed at similar strains ($\gamma \approx 20$) and experimental conditions [4].

The dashed rectangle marked in Fig. 3a shows the presence of very tiny strips within the recrystallized structure (below 1 μm in thickness). Within these strips an interesting microstructure consisting of a few lamellae containing elongated subgrains can be seen (Fig. 3c). Note the large fraction of high angle boundaries in the substructure marked by black lines. The microtexture corresponding to this strip, in particular, also belongs to the γ-fiber (Fig. 3d). One has to be careful to analyze this result. This particular pole figure has a poor statistical basis, since only a few crystallites were taken into account for its automated calculation. However, the microstructure found within these strips support the occurrence of rotational dynamic recrystallization within ASB during the shock-loading experiments.

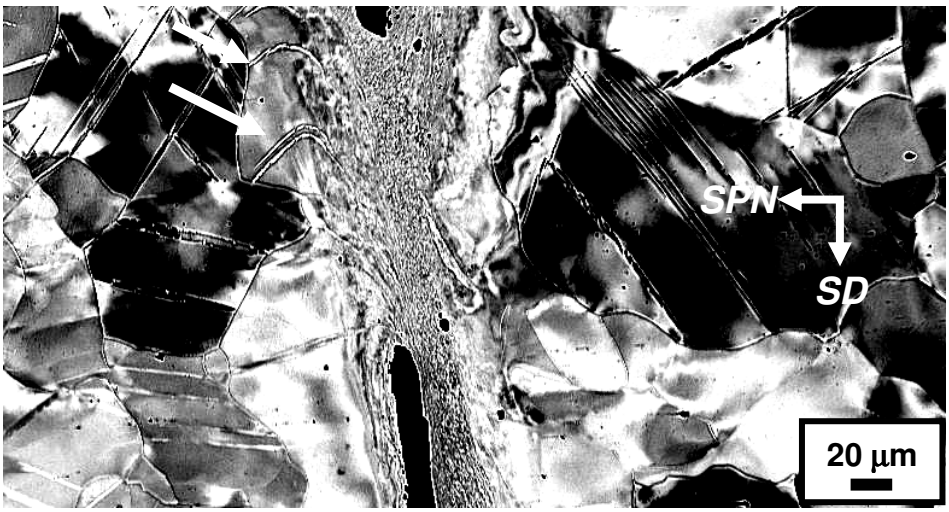


**Fig. 2** – Electron channeling micrograph of the shear region of sample S-1.White arrows indicate bowed deformation twins.

EBSD mappings were also performed in sample S-2 deformed at a lower temperature. Fig. 4a shows the presence of regions with equiaxed grains in the central portion of the ASB as well as a fine lamellar structure. The tiny strips found in sample S-1 are not found anymore. The mean grain size found in this structure was about 0.56 μm, slightly larger than the value of 0.42 determined in sample S-1. Accurate details of the recrystallized structure were obtained with the aid of high-resolution EBSD measurements. The ODF (section $\varphi_2$ = 45°) shown in Fig. 4b reveals a strong <111> γ-fiber and weak α-fiber components. It was calculated based on nearly 3400 grains. These features suggest that rotational dynamic recrystallization is a plausible mechanism to explain the observed microstructures; however, further investigation is needed to validate this hypothesis and to clarify the role played by the temperature rise in the development of the final microstructure. To our knowledge, this is the first set of results showing the formation of a new recrystallized grain structure within ASB in Ti-stabilized IF steels and its corresponding microtexture.

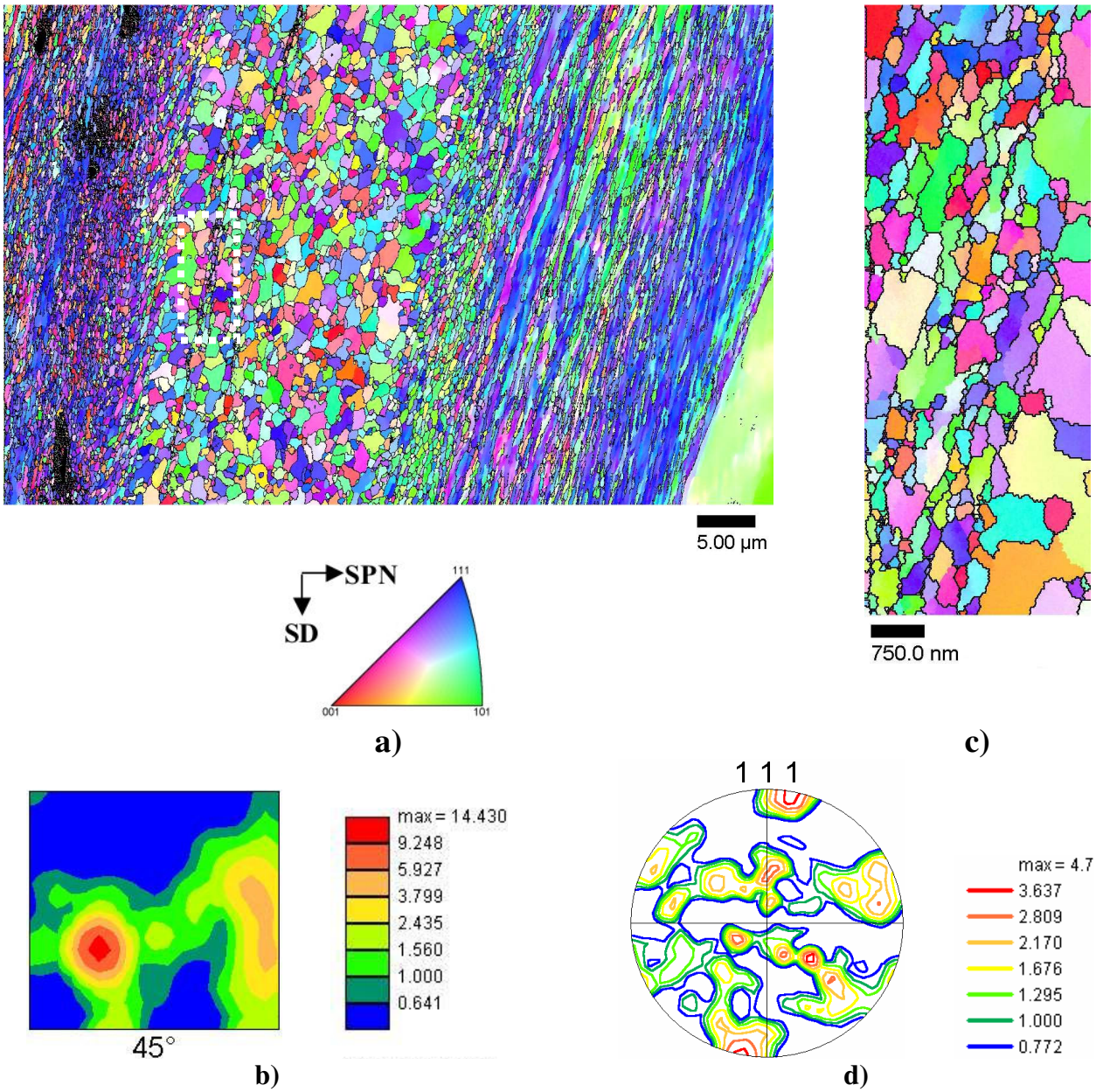


**Fig. 3** – High-resolution OIM of sample S-1: a) general view of the ASB; b) ODF showing $\varphi_2 = 45°$ section; c) enlarged view of the region marked in a); d) microtexture corresponding to the OIM shown in c).

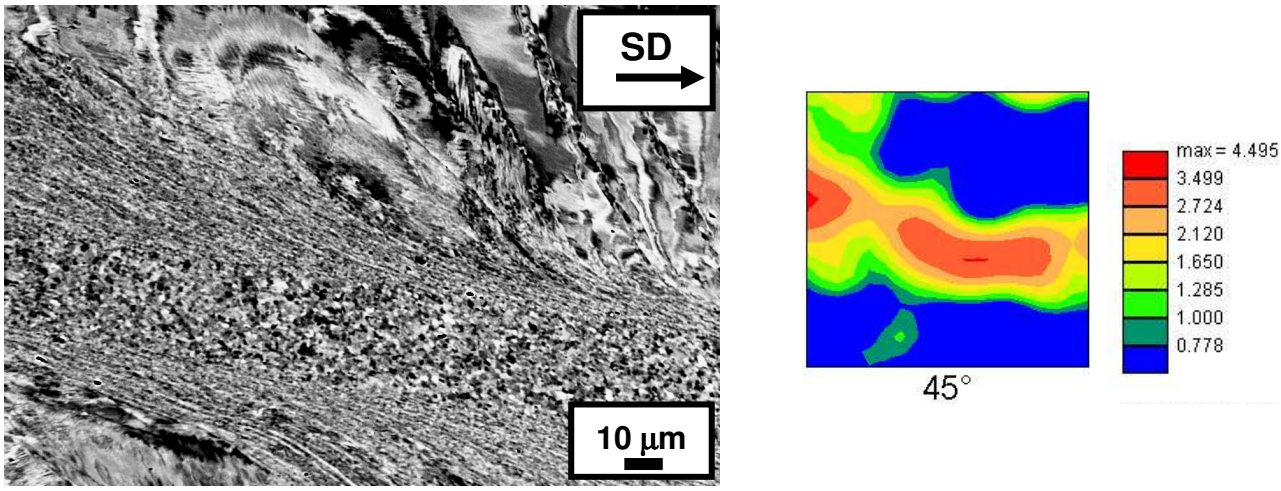


a) b)

**Fig. 4** – SEM micrograph corresponding to sample S-2: a) general view of the microstructure; b) ODF corresponding to the recrystallized grains within the ASB from high-resolution EBSD data.


## Summary

Ti-stabilized IF steel hat-shaped specimens were deformed in a split Hopkinson bar to induce the formation of ASB. The presence of deformation twins bending towards the shear direction strongly suggests that twinning occurs before the flow associated to shear banding. High-resolution EBSD investigated the ultrafine-grained structure developed within ASBs in detail. This new recrystallized grains display a typical γ-fiber texture. Results strongly suggest the occurrence of rotational dynamic recrystallization during straining.



## Acknowledgements

The authors are indebted to FAPESP for the financial support and to Mrs. Katja Angenendt (MPI-E) and Dipl.-Ing. Alice Bastos da Silva (MPI-E) for their kind assistance in FEG-EBSD measurements. The support provided by CNPq (Brazil) to H.R.Z. Sandim is also acknowledged.


## References


[1] S.P. Timothy: Acta metall. Vol. 35 (1987), p. 301.

[2] H.C. Rogers: Ann. Rev. Mater. Sci. Vol. 9 (1979), p. 283.

[3] M.T. Pérez-Prado, J.A. Hines and K.S. Vecchio: Acta mater. Vol. 49 (2001), p. 2905.

[4] M.A. Meyers, Y.B. Xu, Q. Xue, M.T. Pérez-Prado and T.R. McNelley: Acta mater. Vol. 51 (2003), p. 1307.

[5] F.J. Humphreys: J. Mater. Sci. Vol. 36 (2001), p. 3833.

[6] R.K. Ray, J.J. Jonas and R.E. Hook: Int. Mater. Rev. Vol. 39 (1994), p. 129.

[7] J.F.C. Lins and H.R.Z. Sandim: Acta Microscopica Vol. 12-C (2003), p. 273.

[8] Y.J. Chen, M.A. Meyers and V.F. Nesterenko: Mater. Sci Eng. Vol. A268 (1999), p. 70.

[9] M.A. Meyers, O. Vöhringer and V.A. Lubarda: Acta Mater. Vol. 49 (2001), p. 4025.

[10] M.A. Meyers, G. Subhash, B.K. Kad and L. Prasad: Mech. Mater. Vol. 17 (1994), p. 175.

[11] B. Derby: Acta Metall. Vol. 39 (1991), p. 955.

**Textures of Materials - ICOTOM 14**
doi:10.4028/www.scientific.net/MSF.495-497

**An EBSD Investigation on Deformation-Induced Shear Bands in Ti-Bearing IF-Steel under Controlled Shock-Loading Conditions**

doi:10.4028/www.scientific.net/MSF.495-497.393